

Ion-Ion Beam Instability in a Cylindrical Geometry

Noah Hershkowitz,* Thomas Romesser,† Georg Knorr,‡ and Christoph K. Goertz§
Department of Physics and Astronomy, The University of Iowa, Iowa City, Iowa 52242

(Received 21 January 1974)

The ion-ion instability is studied in a cylindrical double-plasma device. Low frequency cylindrical standing waves are found which are one-dimensional in character with frequency proportional to beam velocity. An approximate dispersion relation for the cylindrical standing waves is derived.

Double-plasma (DP) devices have recently been used to study the incoherent ion-ion two-beam instability produced by one-dimensional beams in unmagnetized plasmas.¹⁻⁵ This turbulence is found to be *three*-dimensional in character in agreement with the linear theory of the ion-ion instability⁶⁻⁹ which predicts that the instability depends on $\vec{k} \cdot \vec{v}_b$, where \vec{k} is the *plane*-wave propagation vector and \vec{v}_b is the beam velocity. Although there is an upper limit on v_b beyond which the *one*-dimensional ion-ion instability will not grow, there always will be oblique directions for which the projection of \vec{v}_b on \hat{k} will give growing modes in *three* dimensions. Means *et al.*¹⁰ have recently argued that the observation of turbulence in experiments with *one*-dimensional electrostatic ion acoustic shocks depends fundamentally on this *three*-dimensional property of the instability.

In this Letter we report the production of a coherent ion-ion instability which is essentially one-dimensional in character. This has been accomplished by generating cylindrical *standing* waves which are resonant with ingoing and outgoing beams in a cylindrical DP device at the University of Iowa. This device differs from conventional DP devices¹⁻⁵ in that the cylindrical boundary of the plasma plays a dominant role. A grounded cylindrical screen through which the beam is injected, serves as a well-defined boundary condition (vanishing potential) for the standing waves. In conventional devices¹⁻⁵ the dimensions were such that wave and particle phenomena were *not* significantly affected by the presence of boundaries. The dimensions of those devices were *large* compared to the ion charge-exchange length, the *e* folding distance for ion-acoustic waves, and all wavelengths of interest. In the cylindrical DP device described here the diameter of the plasma is comparable to these lengths.

A description of these standing waves is derived from the Vlasov equation in a cylindrical

geometry. The dependence of the frequencies ω of the instabilities on the beam velocity is shown to be remarkably similar, but not identical, to the results for a strictly one-dimensional ion-ion instability.

The cylindrical DP device, which has recently been used to study cylindrical solitons,¹¹ is shown in Fig. 1. Two *concentric* argon plasmas are separated by an outer negatively biased screen and an inner screen held at ground potential. Plasma within the inner cylinder is produced in an adjacent connected chamber. Typical operating parameters were electron temperature $T_e \approx 1$ eV, ion temperature $T_i \approx 0.1$ to 0.2 eV, average plasma density $n_i \sim 10^8$ to 10^9 cm⁻³, and pressure $\approx 2 \times 10^{-4}$ Torr. A steady-state radially ingoing cylindrical beam is formed by raising the plasma potential in the outer cylinder. Beam density ratios $\eta \equiv n_b/n_i$ are controlled by varying the concentric discharges. The ion charge-exchange length was greater than the inner-cylinder radius.

Energy distribution functions in the inner plasma (region A in Fig. 1) are measured with two energy analyzers with depth-to-area ratios great-

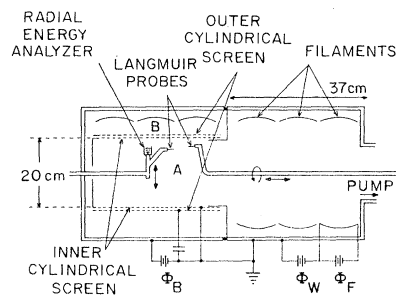


FIG. 1. Cylindrical DP device with two insulated concentric plasmas. The inner plasma is produced in the right half of the device. Beam energy is controlled by varying Φ_B . Φ_F , filament supply voltage; Φ_W filament-to-wall voltage; Φ_B , applied bias voltage. $T_e = 1.0$ eV; $T_i \lesssim 0.2$ eV; $N_0 = 10^8 - 10^9$ cm⁻³; pressure, 2×10^{-4} Torr.

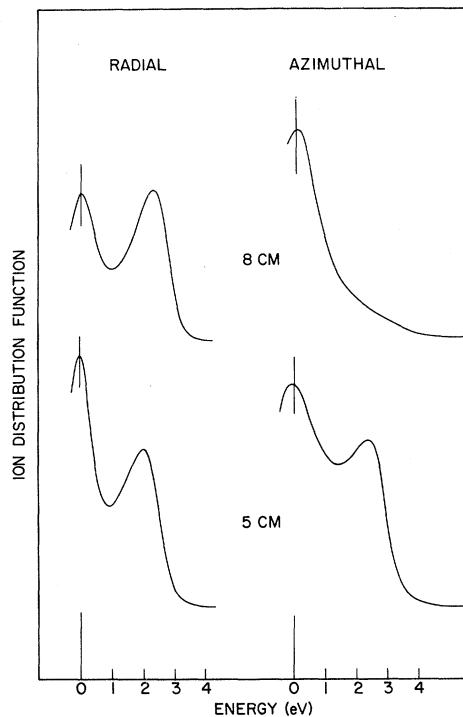


FIG. 2. Typical radial and azimuthal energy-analyzer traces at 5 and 8 cm are shown. Similar traces are observed for radii less than 6 cm indicating the presence of a ring distribution function in velocity space. The absence of an azimuthal beam at 8 cm is apparent. Azimuthal traces are found to be independent of φ . Broadening of these traces is instrumental.

er than 1, whose radial coordinates can be varied. One energy analyzer measures the energy distribution function of particles with velocities in the radial direction, another observes the energy in the φ direction. A third measures outgoing energy distribution functions in the outer plasma (region B in Fig. 1). Typical energy-analyzer traces are shown in Fig. 2. Near the inner screen the beam is seen to be radial. For radii less than 7 cm we find approximately equal radial and azimuthal beam components, indicating that the beam forms a ring in velocity space. The spatial region over which the ring distribution function exists is determined by the beam velocity, and the separation and mesh size of the two concentric screens. The region increases for smaller energies. The presence of a ring distribution function rather than a purely radial beam results in a uniform beam density ($r < 7$ cm) with no steady-state electric field. This facilitates a theoretical description of the instability.

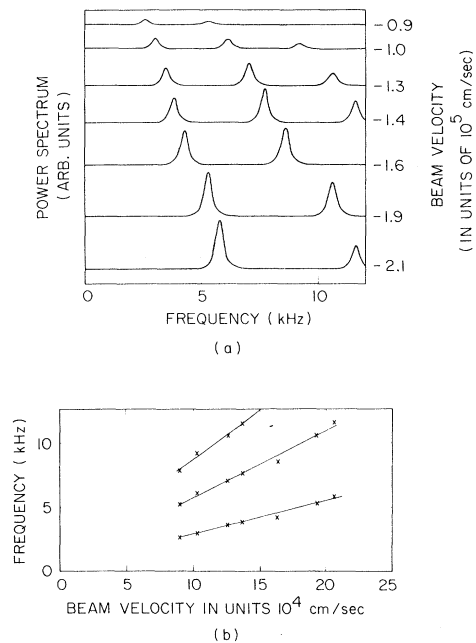


FIG. 3. (a) Power spectra showing the first three harmonics as a function of beam velocity. (b) Frequency versus beam velocity for the three lowest harmonics. No growing modes are observed for $v_b < 0.9 \times 10^5$ cm/sec and for $v_b > 2.2 \times 10^5$ cm/sec.

Instabilities are detected by positively biased Langmuir probes oriented in the axial direction and by the energy analyzers. One Langmuir probe is variable in the radial direction and the other is variable in the φ and axial directions. Langmuir probes indicate that relatively uniform background plasma and beam densities are achieved in this device. Langmuir-probe measurements within the inner cylinder (region A in Fig. 1) showed no φ or z dependence (except near the cylinder ends).

A comparison of signals simultaneously obtained at different positions showed that the instability was *in phase* throughout the inner plasma, demonstrating that standing waves were produced. Therefore it is meaningful to consider power spectra. Typical instability power spectra as a function of beam velocity are shown in Fig. 3(a). For high beam velocities we observe *no instability*. The onset of the instability is seen for a beam energy of approximately 1.0 eV. For beam energies less than approximately 0.2 eV the instability disappears. As the plasma potential of the outer plasma is made less than the potential of the inside plasma we observe incoherent instabilities between the outer cylindrical

screen and the outer walls of the chamber (region B in Fig. 1).

Measurements of the power spectra in the radial direction show that the three lowest frequencies correspond to resonant modes with no nodes, one cylindrical node, and two cylindrical nodes, respectively, further demonstrating cylindrical standing waves. Figure 3(b) shows that ω is roughly proportional to v_b for the first three har-

monics. In addition, the second and third harmonics have approximately 2 and 3 times the frequency of the first. This suggests that $\omega/k_n = \alpha v_b$, with α constant, describes all three modes, with k_n varying approximately with the mode number.

These results can be understood by considering the linear Vlasov equation in cylindrical geometry. The Vlasov equation can be written for one component (ions or electrons) in the following way:

$$\frac{\partial f}{\partial t} + v_r \frac{\partial f}{\partial r} + v_\varphi \frac{\partial f}{\partial \varphi} + \left(\frac{e}{m} E_r + v_\varphi^2 r^{-1} \right) \frac{\partial f}{\partial v_r} + \left(\frac{e}{m} E_\varphi - v_r v_\varphi r^{-1} \right) \frac{\partial f}{\partial v_\varphi} = 0. \quad (1)$$

For a stationary homogeneous equilibrium distribution $f_0(r, v_r, v_\varphi)$ with $\vec{E} = 0$, we find $v_\varphi r^{-1} (v_\varphi \partial f_0 / \partial v_r - v_r \partial f_0 / \partial v_\varphi) = 0$. This means that the zeroth-order distribution function depends only on the magnitude of the velocity, $f_0 = f_0(v) = f_0[(v_r^2 + v_\varphi^2)^{1/2}]$; i.e., the distribution is *concentric* in velocity space and the beam must be a ring. Experimentally, we find such a distribution function extending from the center to within 3 cm of the inner screen for beam energies less than 2 eV.

Perturbing the plasma, we write $f(\vec{r}, \vec{v}, t) = n_0 f_0(v) + f_1(\vec{r}, \vec{v}, t)$, where $f_1(\vec{r}, \vec{v}, t)$ is given by

$$f_1(\vec{r}, \vec{v}, t) = \int_0^t dt_0 \nabla \Phi(\vec{r}_0(\vec{r}, \vec{v}, t - t_0), t_0) \cdot \partial f_0(v) / \partial \vec{v}, \quad (2)$$

with Φ being the electrostatic potential. The time integral is taken along the straight-line orbits of the unperturbed state. In evaluating the time integral we consider the plane-propagating waves $\Phi(\vec{r}, t) = \Phi_0 \exp[i(ax + by - \omega t)] = \Phi_0 \exp[i[kr \cos(\varphi - \alpha) - \omega t]]$. Then the integral in Eq. (2) can be performed to give

$$f_1(\vec{r}, \vec{v}, t) = \frac{e}{m} \Phi(\vec{r}, t) \frac{kv \cos(\theta - \alpha)}{kv \cos(\theta - \alpha) - \omega} \frac{\partial f_0(v)}{v \partial v}. \quad (3)$$

In writing Eq. (3) and the potential we have used the following definitions:

$$x = r \cos \varphi, \quad y = r \sin \varphi, \quad v_x = v \cos \theta, \quad v_y = v \sin \theta, \quad a = k \cos \alpha, \quad b = k \sin \alpha.$$

When calculating the density from Eq. (3) by integrating over v and θ , we note that the dependence of $\cos(\theta - \alpha)$ on α can be suppressed because θ is integrated over all angles. Thus we obtain for the density

$$n(\vec{r}, t) = \int_0^\infty v dv \int_0^{2\pi} d\theta f_1 = (e/m) n_0 \Phi(\vec{r}, t) k^2 G(\omega/k, f_0), \quad (4)$$

with

$$G\left(\frac{\omega}{k}, f_0\right) = k^{-2} \int_0^\infty v dv \int_0^{2\pi} d\theta \frac{\cos \theta}{\cos \theta - \omega/kv} \frac{\partial f_0(v)}{v \partial v}. \quad (5)$$

In order to express the density in cylinder functions we let Φ_0 depend on α , $\Phi_0(\alpha) = (\Phi_\nu/\pi) \exp(i\nu\alpha - \nu\pi/2)$, and integrate over α . A change of the variable α to $w = A + \varphi$ and an appropriate extension of the limits of the integral to infinity produces the integral representation of the Hankel or Bessel functions $Z_\nu(kr) \exp(i\nu\varphi)$. Thus we can write

$$n(r, t) = (e/m) \Phi_\nu Z_\nu(kr) \exp(i\nu\varphi) G. \quad (6)$$

The densities have to be inserted into Poisson's equation,

$$-\nabla^2 \Phi = 4\pi \sum_j e_j n_j. \quad (7)$$

We note that $Z_\nu(kr) \exp(i\nu\varphi)$ is an eigenfunction of the Laplacian. This shows that cylinder functions are eigenfunctions of the beam-plasma system. For the boundary conditions of the experiment, $\Phi = 0$ on boundary, we obtain directly $\nu = 0$, $kR = \alpha_{0\mu}$, where $\alpha_{0\mu}$ is the μ th zero of the Bessel function $J_0(\rho)$. It is important to notice that these are the only nonsingular solutions and they represent standing

waves. The dispersion relation is found from Eqs. (7), (6), and (5):

$$D(k, \omega) = 1 - \sum_j \omega_{pj} G_j = 1 - \sum_j \omega_{pj}^2 k^{-2} \int_0^\infty v dv \int_0^{2\pi} d\theta \frac{kv \cos \theta}{kv \cos \theta - \omega} \frac{\partial f_{0j}(v)}{v \partial v} = 0. \quad (8)$$

Note that $k = \alpha_{0\mu}/R$. k is not a *plane*-wave propagation vector.

We consider now a background plasma with Maxwellian ion and electron distributions with $T_e \gg T_i$. In addition we have a radial influx of ions of velocity v_b , which can approximately be described by $f_b(v) = (n_b/2\pi v_b) \delta(v - v_b)$. From the Penrose criterion it follows that for small v_b the system is stable as well as for very large v_b . Both effects have been observed experimentally [compare Fig. 3(b)]. From the assumed distribution functions we find for very small ion beam density ($\eta \ll 1$) and for $v_b \neq (kT_e/m_i)^{1/2} \equiv c_s$

$$\omega = +kv_b \left[1 + \frac{1}{2} \eta^{2/3} \exp(2\pi i/3) c_s^{4/3} (v_b^2 - c_s^2)^{-2/3} \right].$$

For the case of resonance ($v_b = c_s$) we find $\omega = +kv_b \left[1 + \frac{1}{2} \eta^{2/5} \exp(2\pi i/5) \right]$. The experimental proportionality of ω with v_b is evident from Fig. 3(b) which corresponds to $\eta \approx 0.2$.

In conclusion we have shown that low-frequency cylindrical standing waves which depend only on r are produced by the ion-ion beam instability in a cylindrical DP device. We have shown that their frequency is roughly proportional to the beam velocity. We believe that this is the first time that a coherent ion-ion beam instability has been observed. We ascribe this to the high symmetry of the experiment which substantially reduces the off-axis modes. We have derived a dispersion relation for the coherent cylindrical-standing-wave instability from the appropriate Vlasov equations for the cylindrical geometry. This predicts unstable standing waves with ω/k_n proportional to v_b rather than traveling waves.

We are indebted to David Montgomery for advice, assistance, and enlightening discussions. We are grateful to Professor I. Alexeff for a very thorough and critical discussion of this paper. We would like to acknowledge helpful discussions with Professor G. Joyce. In addition we thank Alfred Scheller for construction of much of the apparatus.

*Present address: Department of Physics, University of California, Los Angeles, Calif. 90024.

†Work supported in part by the National Aeronautics and Space Administration under Grant No. NGL-16-001-043.

‡Work supported in part by the U. S. Atomic Energy Commission under Contract No. AT(11-1)-2059.

§Work supported in part by the National Science Foundation under Grant. No. GA-31676.

¹R. J. Taylor, D. R. Baker, and H. Ikezi, Phys. Rev. Lett. **24**, 206 (1970).

²R. J. Taylor, K. R. MacKenzie, and H. Ikezi, Rev. Sci. Instrum. **43**, 1675 (1972).

³A. Y. Wong and R. W. Means, Phys. Rev. Lett. **27**, 973 (1971).

⁴R. A. Stern and J. F. Decker, Phys. Rev. Lett. **27**, 1266 (1971).

⁵R. J. Taylor and F. V. Coroniti, Phys. Rev. Lett. **29**, 34 (1972).

⁶B. D. Fried and A. Y. Wong, Phys. Fluids **9**, 1084 (1966).

⁷T. M. O'Neil and J. H. Malmberg, Phys. Fluids **11**, 1754 (1968).

⁸D. W. Forslund and C. R. Shonk, Phys. Rev. Lett. **25**, 281 (1970).

⁹S. Abas and S. P. Gary, Plasma Phys. **13**, 262 (1971).

¹⁰R. W. Means, F. V. Coroniti, A. Y. Wong, and R. B. White, Phys. Fluids **16**, 2304 (1973).

¹¹N. Hershkowitz and T. Romesser, Phys. Rev. Lett. **32**, 581 (1974).